Probabilistic tsunami hazard in the Mediterranean Sea

Mathilde B. Sørensen,[1,2] Matteo Spada,[3] Andrey Babeyko,[4] Stefan Wiemer,[3] and Gottfried Grünthal[4]

[1] Estimating the occurrence probability of natural disasters is critical for setting construction standards and, more generally, prioritizing risk mitigation efforts. Tsunami hazard in the Mediterranean region has traditionally been estimated by considering so-called "most credible" scenarios of tsunami impact for limited geographical regions, but little attention has been paid to the probability of any given scenario. We present here the first probabilistic estimate of earthquake-generated tsunami hazard for the entire Mediterranean Sea. We estimate the annual probability of exceeding a given tsunami amplitude at any coastal location in the region by applying a Monte Carlo based technique. Earthquake activity rates are estimated from the observed seismicity, and tsunami impact is derived from deterministic tsunami wave propagation scenarios. The highest hazard is in the eastern Mediterranean owing to earthquakes along the Hellenic Arc, but most of the Mediterranean coastline is prone to tsunami impact. Our method allows us to identify the main sources of tsunami hazard at any given location and to investigate the potential for issuing timely tsunami warnings. We find that the probability of a tsunami wave exceeding 1 m somewhere in the Mediterranean in the next 30 years is close to 100%. This underlines the urgent need for a tsunami warning system in the region.

Citation: Sørensen, M. B., M. Spada, A. Babeyko, S. Wiemer, and G. Grünthal (2012), Probabilistic tsunami hazard in the Mediterranean Sea, *J. Geophys. Res.*, *117*, B01305, doi:10.1029/2010JB008169.

1. Introduction

[2] The series of deadly tsunamis in recent years, such as the extreme events in Sumatra (2004), Chile (2010), and most recently Japan (2011), is a chilling reminder of this natural disaster's destructive power. While earthquakes allow at best several seconds of warning, the time available for issuing a tsunami warning ranges from minutes to many hours. It is thus technologically possible to warn people of the danger, and local and regional tsunami warning systems are being constructed or enhanced around the globe to mitigate the risk.

[3] In the past 2500 years, the Mediterranean countries have experienced several catastrophic tsunamis. The most well known occurred in 365, 1303, and 1908; the first two were caused by earthquakes in the Hellenic Arc, and the third occurred in the Messina Strait. Other devastating events occurred in 373 B.C. and 1748 in the Gulf of Corinth and in 1783 in the Messina strait. The most recent destructive tsunamis occurred in the Aegean Sea in 1956 with runup heights reaching 25 m [*Papazachos et al.*, 1985] and north of Algeria in 2003 with runup heights up to 2 m in the Balearic Islands [*Alasset et al.*, 2006]. Each of these

tsunamis was generated by a strong earthquake [*Soloviev*, 1990; *Papadopoulos and Fokaefs*, 2005]. Large tsunamis have also been generated by volcanic eruptions, such as the 1650 eruption of the Thera (Santorini) volcano in the southern Aegean Sea. Thera also caused a remarkably strong tsunami around 1600 B.C. [*Friedrich et al.*, 2006] and has been cited as contributing to the destruction of the Minoan civilization [*Soloviev*, 1990]. The European GITEC-TWO [*Tinti et al.*, 2001] tsunami catalog contains 94 reliably assessed earthquake-generated tsunami events during the last 2500 years. A tsunami warning system for the Mediterranean region has been discussed in earnest since the 2004 Sumatra event claimed more than 200,000 lives, but so far the implementation of such a system has not been initiated.

[4] Tsunami hazard has traditionally been studied by simulating the effect of "worst-case" or "most credible" scenario events with little emphasis on the probability of the scenario events [e.g., *Tinti and Armigliato*, 2003; *Hébert et al.*, 2005; *Paulatto et al.*, 2007; *Lorito et al.*, 2008; *Shaw et al.*, 2008]. Although such scenarios can be extremely useful for response planning, knowledge of the probability of occurrence of an event is crucial for planning risk mitigation efforts (especially when considering multiple hazards), for defining building design specifications and for insurance pricing. Probabilistic tsunami hazard assessment (PTHA) has therefore received increased attention in the recent years [e.g., *Geist and Parsons*, 2006; *Power et al.*, 2007; *Thio et al.*, 2007]. The probabilistic treatment of the problem allows us to study the relative contributions of large and small events to the hazard.

[1]Department of Earth Science, University of Bergen, Bergen, Norway.
[2]Formerly at GFZ German Research Centre for Geosciences, Potsdam, Germany.
[3]Swiss Seismological Service, ETH Zürich, Zürich, Switzerland.
[4]GFZ German Research Centre for Geosciences, Potsdam, Germany.

Furthermore, probabilistic hazard estimates can be deaggregated to identify critical scenarios for a given site and to estimate, at a given site, the time available for issuing warnings in a future early warning system. The identified critical scenarios can following be studied in more detailed, high-resolution deterministic studies where regional and local propagation effects can be accounted for. The large difference to previous deterministic studies will in this case be that the occurrence probability of the considered event is known.

2. Probabilistic Tsunami Hazard Assessment

[5] We obtained a probabilistic estimate of tsunami hazard in the Mediterranean region by applying a Monte Carlo technique similar to that commonly applied for seismic hazard assessment [*Wiemer et al.*, 2009]. We consider in this study only earthquake-generated tsunamis. Whereas other sources (volcanic eruptions, landslides or meteor impacts) can also generate devastating tsunamis, stable statistical models describing the occurrence of these phenomena are currently not available. Earthquakes are expected to cause at least 75% of the tsunami events in the Mediterranean Sea [*Soloviev*, 1990]. The possibility of other sources should, however, not be neglected and it is recommended to focus future research on a statistical description of their spatial and temporal occurrence patterns.

[6] To estimate the tsunami hazard, we first created a collection of all potentially tsunamigenic earthquake sources and the corresponding relevant seismicity parameters. We used this information to construct a synthetic catalog of potentially tsunamigenic earthquakes. For each event in the synthetic catalog, we calculated the corresponding tsunami propagation scenario and the overall hazard is described by the combined effect of all scenarios. We constructed a hazard curve for each forecast point by calculating the frequency with which predefined tsunami amplitude thresholds are exceeded in the tsunami scenarios.

2.1. Zonation

[7] We identified source regions of potentially tsunamigenic earthquakes considering the European-Mediterranean Earthquake Catalog (G. Grünthal and R. Wahlström, The European-Mediterranean Earthquake Catalog (EMEC), submitted to *Journal of Seismology*, 2011). Our aim with the zonation is to cover all areas that may generate a tsunamigenic earthquake, that is, an earthquake causing sufficient vertical sea-bottom displacement to initiate a tsunami wave. The question of whether the specific earthquakes within a given zone are indeed tsunamigenic is determined by their sea bottom displacement which is used as input to the tsunami propagation modeling. If the sources are defined in accordance with the tectonic regime at a given location, the source models for earthquakes will lead to insignificant sea bottom displacements for nontsunamigenic earthquake sources. As a consequence, we include mainly offshore areas in the zonation, but also go some distance inland to assure that potentially tsunamigenic events in the coastal areas are not excluded.

[8] Our source zone model for the Mediterranean region consists of 21 source zones. These sources are chosen to be small enough to represent regions of relatively homogeneous earthquake activity rates and faulting regimes while at the

same time being sufficiently large that the earthquake catalog contains enough events within each zone to perform a stable statistical analysis for the source zone characteristics. For parts of the Mediterranean region (for example the Aegean region and parts of Italy), quite detailed information is available which would allow for a more detailed zonation. However, we have chosen in this study to apply a zonation that is homogeneous in terms of the level of detail considered. The source zones are shown in Figure 1.

[9] Activity rates are represented through the ν and β values in the truncated Gutenberg-Richter relation [*Cosentino et al.*, 1977; *Weichert*, 1980]:

$$\nu(M) = \nu(M_{\min})\left(1 - \frac{1 - e^{-\beta(M - M_{\min})}}{1 - e^{-\beta(M_{\max} - M_{\min})}}\right), \qquad (1)$$

where $\nu(M)$ is the annual number of events with magnitude $\geq M$ and $M_{\min}$ and $M_{\max}$ are minimum and maximum magnitude considered, respectively. We determined $\nu(M_{\min})$ and β for each source zone on the basis of the complete part of the EMEC catalog by applying the maximum likelihood method of *Weichert* [1980]. The completeness time was determined for each source zone separately to allow for spatial variations in catalog completeness. For each magnitude class of half a magnitude unit, a staircase plot was generated showing the cumulative number of events with time. The completeness time was set to the time from which the staircase curve has a constant slope, indicating a constant seismicity rate. The obtained completeness times are listed in Table 1, and the parameters are listed for each source zone in Table 2.

[10] Several methods have been developed to estimate the maximum earthquake magnitude to occur in a given source zone [e.g., *Electric Power Research Institute*, 1994; *Budnitz et al.*, 1997]. Considering the long duration of the earthquake catalog, the high-seismicity regions are expected to be covered with several seismic cycles, and we therefore decided to simply round to the nearest 0.5 magnitude unit higher than the maximum observed magnitude. In order to allow for rare strong events in low-seismicity regions, an overall minimum $M_{\max}$ of 7.5 was defined. In a few cases, the estimate has been further modified for general consistency. The maximum observed magnitudes and the assigned $M_{\max}$ values are listed in Table 2.

[11] The tsunamigenic potential of an earthquake is strongly dependent on event depth and focal mechanism. In this respect, dip-slip earthquakes in general lead to much larger vertical sea bottom displacements than strike-slip events, and are therefore generally much more tsunamigenic. Strike-slip events, on the other hand, rarely generate tsunamis directly. It was therefore necessary to assign faulting regimes and event depths to each source zone. Some of the source zones generate earthquakes with different types of faulting mechanisms, and we therefore assigned more than one faulting regime to some of the zones, with an associated percentage of events falling within each regime. For the Italian region, very detailed information about active faults and their rupture properties is available in the DISS3 database [*DISS Working Group*, 2009], and this information was adopted directly in this study. For the remaining regions, focal mechanisms from the global CMT catalog (www.globalcmt.org) have been studied. For each region, the CMT solutions were divided
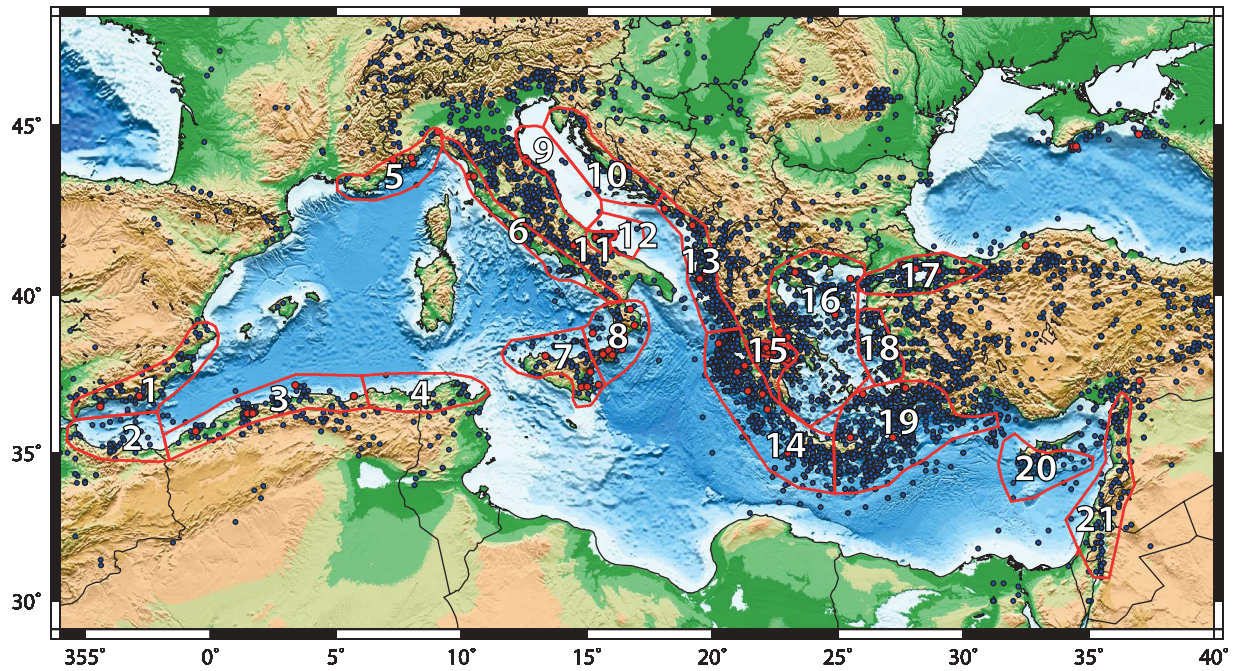
Figure 1. Zonation used for tsunami hazard assessment. Numbers refer to zone numbers in Tables 1 and 2. Blue dots are earthquakes with $M \geq 5$ from the European-Mediterranean Earthquake Catalog (EMEC), and red dots are historical tsunami events [*Tinti et al.*, 2001].

into groups of similar mechanisms. For each group, average values of strike, dip and rake, and their associated standard deviations were calculated, and the zone was assigned characteristic faulting regimes in the range mean ± one standard deviation. The percentage of events with the given faulting regime was defined on the basis of the number of events in the corresponding group. Hypocenter depth information was taken from the DISS3 database for the Italian region and from the EMEC catalog in a similar manner to the focal mechanisms for the remaining regions. The assigned faulting and depth information is listed in Table 2.

2.2. Synthetic Catalog

[12] Using the derived information about the source zones, we constructed a synthetic earthquake catalog of 100,000 years duration, which has the same distribution of magnitudes and faulting regimes as the observed catalog. The synthetic catalog contains a total of 84,920 earthquakes with $M \geq 6.5$, a 10,000 year subset of the catalog is shown in Figure 2. The synthetic earthquake catalog was generated following the approach described by, for example, *Cornell* [1968] and *Reiter* [1990]. The basic idea is to

Table 1. Completeness Times Obtained for Each Source Zone by Analyzing the Temporal Evolution of Seismicity Rates in the Earthquake Catalog

Number	Name	3.5	4.0	4.5	5.0	5.5	6.0	6.5	7.0	7.5	8.0	8.5
1	Southeastern Spain	1940	1920	1900	1900	1900	1450	1350	1350	1350	1350	-
2	Northern Morocco	2000	1998	1925	1900	1900	1750	1750	-	-	-	-
3	Northern Algeria	2002	2001	1998	1985	1985	1850	1775	1700	1700	-	-
4	Northern Tunisia	2003	2003	1910	1905	1905	1905	1905	412	-	-	-
5	Ligurian coast	1965	1965	1840	1550	1550	1550	1300	-	-	-	-
6	Western Italy	2006	2005	1860	1700	1500	1500	-	-	-	-	-
7	Sicily	2002	2002	1860	1860	1700	1700	1100	1100	1100	-	-
8	Calabria	2003	2003	1880	1840	1790	1700	1400	1400	-	-	-
9	Eastern Italy	2006	1900	1900	1820	1220	1220	1100	-	-	-	-
10	Western Croatia	1950	1900	1890	1840	1840	1840	1250	-	-	-	-
11	Gargano, onshore	2005	2005	1840	1840	1790	1520	1400	-	-	-	-
12	Gargano, offshore	2003	2003	1900	1840	1790	1414	-	-	-	-	-
13	Western Albania	1996	1995	1963	1960	1915	1850	1800	1700	-	-	-
14	Western Hellenic Arc	-	1965	1965	1950	1930	1900	1630	1630	1500	1500	300
15	Gulf of Corinth	-	1965	1960	1950	1920	1900	1850	1700	-	-	-
16	Aegean Sea	-	1965	1965	1950	1900	1850	1800	1800	1800	-	-
17	Marmara Sea	1995	1995	1985	1970	1900	1850	1850	1700	1300	-	-
18	Western Anatolia	2000	1972	1972	1965	1915	1850	1850	1850	-	-	-
19	Eastern Hellenic Arc	1996	1990	1970	1960	1915	1900	1890	1750	1700	1000	-
20	Cyprus	1995	1993	1985	1985	1930	1920	1100	−90	−90	-	-
21	Dead Sea Fault area	1980	1980	1980	1980	1890	1700	950	−200	−854	-	-

Table 2. Recurrence Parameters, Maximum Earthquake Magnitude, and Faulting Regimes Assigned to the Source Zones[a]

Number	Name	M_{obs}	M_{max}	β	$\nu(M5)$	Depth (km)	Strike (deg)	Dip (deg)	Rake (deg)	Percentage of Events
1	Southeastern Spain	7.8	8.0	1.89	0.23	0–40	300–330	35–55	(−140)–(−100)	50
						0–40	10–30	35–55	(−140)–(−100)	50
2	Northern Morocco	6.7	7.5	2.46	0.12	1–25	40–110	30–60	80–110	100
3	Northern Algeria	7.3	8.0	2.42	0.82	1–25	40–110	30–60	80–110	100
4	Northern Tunisia	7.0	7.5	2.03	0.16	1–25	40–110	30–60	80–110	100
5	Ligurian coast	6.3	7.5	2.16	0.06	3–10	250–270	25–35	80–100	100
6	Western Italy	5.9	7.5	2.23	0.17	1–10	300–330	30–46	(−100)–(−80)	50
						1–12	325–345	55–65	(−100)–(−80)	50
7	Sicily	7.4	8.0	2.19	0.28	2–18	220–280	30–60	60–120	16
						3–10	250–290	40–60	85–135	12
						3–10	260–320	20–40	75–125	12
						3–10	220–260	20–40	80–100	12
						3–15	50–70	40–50	60–90	12
						1–25	140–170	70–90	(−180)–(−140)	12
						10–23	355–15	60–90	(−10)–30	12
						10–23	10–30	70–90	(−10)–10	12
8	Calabria	7.2	7.5	2.05	0.31	11–50	180–250	20–40	80–100	20
						3–12	145–205	20–40	80–100	17
						3–12	20–40	24–40	(−110)–(−80)	9
						3–12	290–310	60–80	(−150)–(−120)	9
						3–11	20–40	20–40	(−100)–(−80)	9
						3–12	110–130	60–80	(−60)–(−30)	9
						3–15	90–110	70–90	(−30)–10	9
						1–10	160–200	50–70	(−100)–(−80)	9
						1–10	150–170	55–65	(−100)–(−80)	9
9	Eastern Italy	6.5	7.5	3.11	0.10	3–7	80–100	70–90	170–(−130)	12
						3–7	120–140	25–35	80–100	11
						3–8	120–140	25–35	80–100	11
						3–7	110–140	30–36	90	11
						3–7	110–150	30–46	80–100	11
						2–7	120–150	30–46	80–100	11
						3–7	120–150	30–46	80–100	11
						3–8	145–175	30–50	80–110	11
						11–20	110–160	30–46	80–100	11
10	Western Croatia	6.5	7.5	1.73	0.21	2–22	275–323	15–31	55–117	100
11	Gargano, onshore	6.7	7.5	2.69	0.12	6–25	250–270	80–90	(−180)–(−120)	34
						0–25	260–290	80–90	(−160)–(−130)	33
						11–23	260–280	70–90	170–(−170)	33
12	Gargano, offshore	5.8	7.5	2.23	0.04	1–25	90–100	80–90	160–(−170)	100
13	Western Albania	7.0	7.5	1.93	1.45	1–15	290–330	30–46	60–100	25
						1–12	320–350	30–46	70–110	25
						1–12	310–350	30–46	70–110	25
						1–12	310–330	30–46	70–100	25
14	Western Hellenic Arc	8.3	8.5	1.84	3.85	5–70	250–320	30–40	50–100	70
						3–20	10–40	50–80	150–170	30
15	Gulf of Corinth	7.0	7.5	1.70	0.51	7–31	28–148	47–67	(−130)–(−58)	100
16	Aegean Sea	7.5	8.0	1.84	2.20	6–34	68–92	34–60,	(−129)–(−63)	31
						6–34	70–76	57–89	(−179)–(−145)	9
						6–34	252–286	40–54	(−139)–(−69)	13
						6–34	235–251	69–77	(−174)–(−156)	31
						6–34	216–250	64–88	160–(176)	16
17	Marmara Sea	7.5	8.0	1.73	0.83	0–20	227–283	52–90	163–(−157)	50
						0–20	64–112	54–88	146–(−112)	50
18	Western Anatolia	7.1	7.5	2.19	1.16	2–26	140–154	62–86	(−36)–(−6)	64
						2–26	253–261	45–61	(−133)–(−121)	36
19	Eastern Hellenic Arc	8.0	8.5	2.44	5.77	10–66	248–122	36–80	(−23)–27	35
						10–66	253–277	51–79	70–104	27
						10–66	341–37	43–69	(−104)–(−58)	16
						10–66	349–113	55–89	56–116	16
						10–66	12–66	39–81	148–(−150)	6
20	Cyprus	7.3	7.5	1.98	0.22	6–30	355–155	57–85	(−44)–100	60
						6–30	315–11	31–81	71–123	40
21	Dead Sea Fault area	7.5	8.0	1.66	0.28	3–19	328–126	50–62	(−81)–13	100

[a]Value $\nu(M5)$ is the annual number of earthquakes with $M \geq 5$, M_{obs} is the maximum observed magnitude within the zone, and M_{max} is the assigned maximum magnitude. For source zones that generate earthquakes with different types of faulting mechanisms, more than one faulting regime has been assigned, and the "Percentage of Events" column gives the percentage of events falling within each regime.
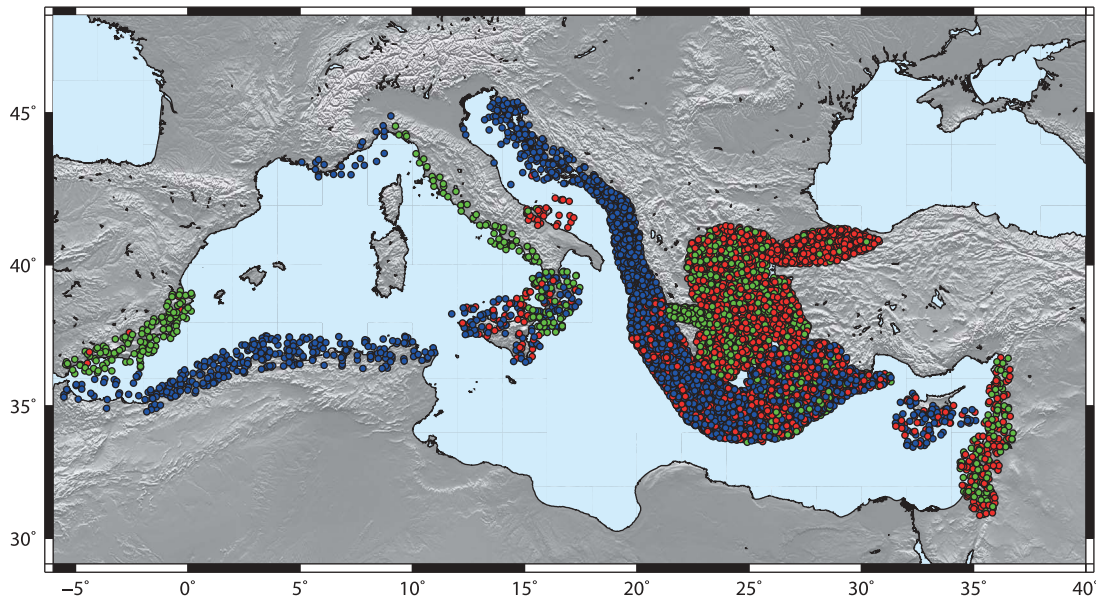
Figure 2. A 10,000 year subcatalog of the synthetic earthquake catalog. Events are color coded according to focal mechanism (red for strike-slip, green for normal, and blue for reverse).

expand data from an observational period, normally less than 2,000 years, which is short with respect to the rareness of studied events, onto a long time span, in our case 100,000 years. The spatial distribution of earthquake hypocenters is assumed to be random within a volume defined by the 2D geometry of the source zone (latitude and longitude) and the source zone depth range. The number of events in a given source zone is determined from the ν value (Table 2). Magnitudes are sampled from a double-truncated Gutenberg-Richter magnitude recurrence curve [*Cosentino et al.*, 1977; *Weichert*, 1980], modeled with a slope β and a maximum magnitude M_{max}. The events are furthermore distributed randomly in time, following a Poissonian distribution.

[13] To each synthetic event was also assigned a strike, dip and rake angle, randomly drawn from the prescribed distribution derived from the observed data. Rupture length and rupture width were computed from the event magnitude following empirical relationships [*Wells and Coppersmith*, 1994].

2.3. Tsunami Propagation Scenarios

[14] For each event in the synthetic catalog, we calculated the corresponding tsunami propagation scenario and estimated peak coastal tsunami amplitude (PCTA) at 466 coastal locations (forecast points) around the Mediterranean. A uniform slip derived from earthquake moment magnitude with the help of empirical relations for rupture dimensions (see above) was assumed on a fault plane centered at the given hypocenter. The corresponding sea bottom displacement, based on the analytical solution of *Okada* [1985], was used as input to a tsunami wave propagation scenario.

[15] Tsunami wave propagation was solved at a 2 arc minute bathymetric grid derived from the 30 arc seconds General Bathymetric Chart of the Oceans (GEBCO) bathymetry model (The GEBCO_08 Grid, version 20100927, available at http://www.gebco.net, 2008). Each scenario was integrated

for 240 minutes model time to ensure that the tsunami reaches all the coasts of the Mediterranean basin. Wave propagation was computed in the linear approximation of the long-wave theory in spherical coordinates. The applied numerical scheme follows the well-known TUNAMI-F1 algorithm [*Intergovernmental Oceanographic Commission*, 1997], and is leapfrog explicit time-stepping on a staggered finite-difference grid. Boundary conditions presume full reflection along shorelines.

[16] Solving the linear long-wave equations is computationally very efficient, which allowed us to calculate tens of thousands of scenarios from the synthetic earthquake catalog in a short time. However, this approximation is no longer valid in coastal areas with water depths shallower than ~50 m [*Shuto*, 1991], where the nonlinear bottom friction and advection terms become nonnegligible. This fact, combined with the rather coarse bathymetry and topography resolution (2 arc min corresponds to ~3.6 km grid step), did not allow us to calculate coastal runups directly. Instead, we accepted the approach employed and extensively verified by the Japanese tsunami early warning system [*Kamigaichi*, 2009]. In this approach, peak offshore tsunami amplitudes are first computed at some offshore positions (typically, in 50–100 m water depth) and then extrapolated into the peak coastal tsunami amplitudes (PCTA) using the Green's law accounting for wave shoaling.

[17] *Kamigaichi* [2009] found that thus derived PCTAs agree well with the means (and medians) of tsunami amplitudes computed directly at a coastline at a much finer mesh in each coastal subsection. In this respect, extrapolated PCTAs can be considered as representative estimates of the tsunami impact at the coast. As also noted by *Kamigaichi* [2009], this approach cannot discriminate between direct and reflected waves and, hence, may somehow overestimate PCTAs. An example of a scenario for a *M*8.5 earthquake in the Hellenic Arc is presented in Figure 3.
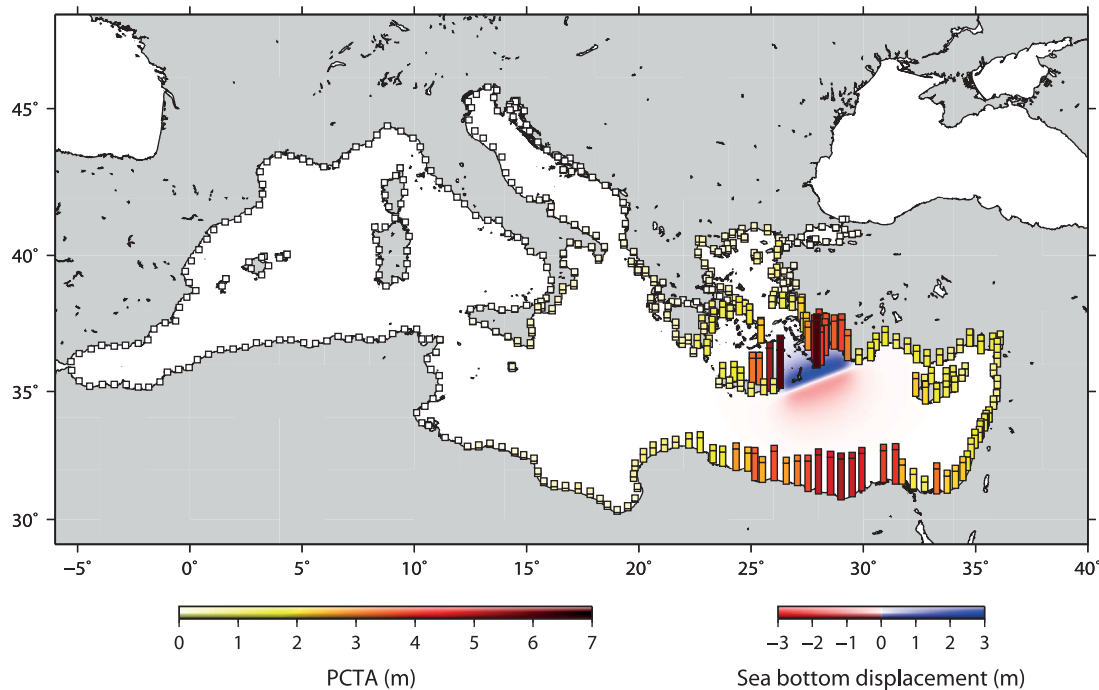
Figure 3. Tsunami propagation scenario for a $M = 8.5$ earthquake in the eastern Hellenic Arc.

2.4. Generation of Hazard Results

[18] At a given site, the annual probability of exceeding a given PCTA was determined by studying all synthetic tsunami propagation scenarios and counting the number of scenarios where the given PCTA was exceeded at the site of interest. Dividing the number of exceedances by the duration of the synthetic catalog (i.e., 100,000 years) then gives the annual exceedance probability.

[19] The uncertainty associated with a given hazard curve is expressed theoretically in terms of the range of possible tsunami heights corresponding to the annual probability of exceedance, defined using a theoretical cumulative normal distribution function within 2σ. In this study, results are presented as the median value, as well as the 15th and 85th percentiles. Uncertainties arise owing to uncertainty in both input parameters (e.g. zonation, activity rates, faulting regimes, estimation of sea bottom displacement etc.) and wave propagation calculations (bathymetry, estimation of PCTA etc). The degree of variability among these parameters differs and is difficult to assess directly. However, more detailed knowledge about the tectonics in the Mediterranean region and the associated earthquake activity can help reducing the degree of epistemic uncertainty in the input data. In order to constrain better the uncertainties and to identify the relative contributions of different sources of uncertainty, a systematic sensitivity study will be necessary. Such a study is planned for the near future.

3. Tsunami Hazard Results

[20] The PTHA results can be expressed either as hazard curves or as hazard maps. The hazard curve for a given site presents the annual probability of exceedance as a function of PCTA. Hazard maps can present either the PCTA corresponding to a fixed annual probability or the probability of exceeding a fixed PCTA threshold in some given time period.

[21] In Figure 4, we present the hazard curves for selected locations in the Mediterranean region. The curves show that the hazard varies greatly throughout the region, but they also indicate that all sites can experience tsunami waves exceeding 1 m when considering sufficiently low probability levels. We emphasize that our results are a minimum estimate of the tsunami hazard because we only considered earthquake-generated tsunamis.

[22] Figure 4 also shows two examples of the uncertainty associated with our hazard curves, expressed in terms of the 15th and 85th percentiles. The relatively high variability is common for probabilistic assessment of natural hazards and is related to the relatively short time coverage of the observed catalog and uncertain knowledge of regional geology and tectonics. Furthermore, errors are associated with each calculation step of the PTHA method. A greater concern related to the uncertainties in the hazard assessment is that owing to the finite duration of the synthetic catalog, it will contain only a subset of the events which could potentially occur in the Mediterranean region. In this regard, it must be investigated whether the hazard results are sensitive to the choice of subset, that is, to the choice of random seed in the synthetic catalog generation. In order to test this, the synthetic catalog has been split into 10 subcatalogs of 10,000 years duration and hazard curves have been derived for each of these subcatalogs. The curves obtained for selected sites are presented in Figure 5. It is found that the hazard curves are extremely stable to the choice of synthetic catalog, confirming that the chosen catalog duration of 100,000 years is sufficient to derive stable hazard curves.

[23] Hazard maps showing PCTA corresponding to a fixed annual probability have been sampled from the median
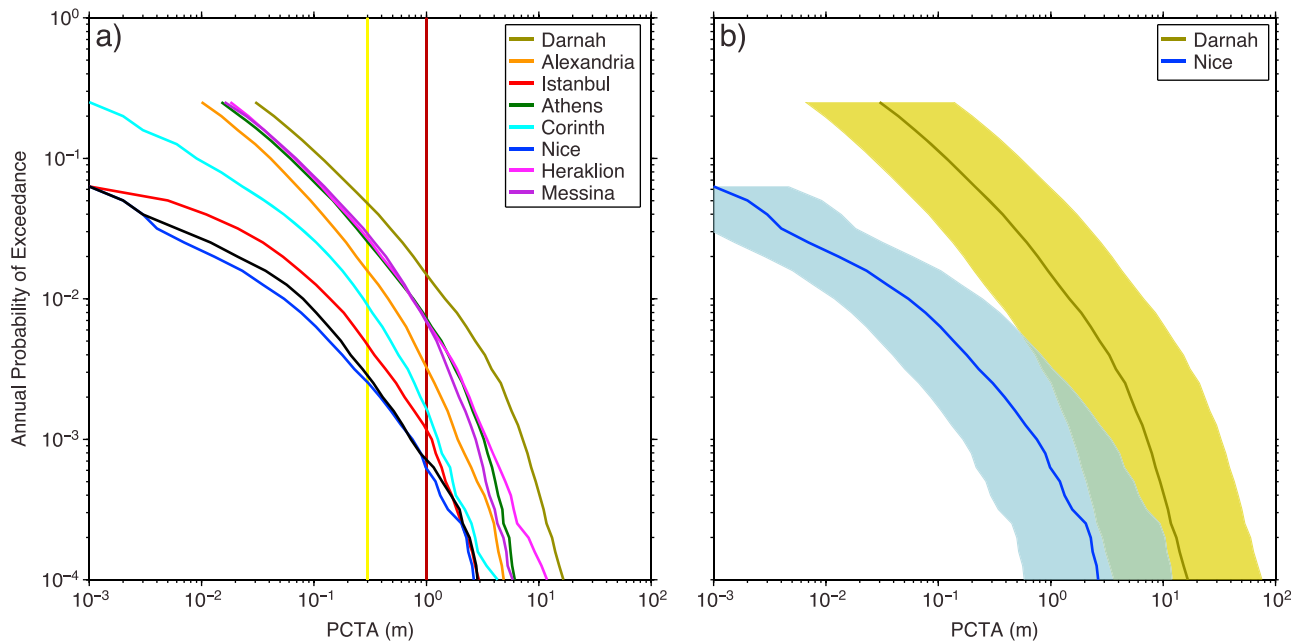
Figure 4. (a) Probabilistic tsunami hazard curves for selected locations along the Mediterranean coastline. Vertical bars mark peak coastal tsunami amplitude (PCTA) of 30 cm and 1 m, which are considered roughly the limits defining a damaging and devastating tsunami, respectively. (b) Uncertainty ranges, spanned by the 15th and 85th percentiles, of the hazard curves for the sites Nice and Darnah.

hazard curves. Such maps are presented for different annual probabilities in Figure 6. The maps show that the distribution of the hazard is relatively unaffected by the annual probability, with tsunami amplitudes increasing with decreasing probability level, as expected.

[24] At relatively short time scales (e.g., an annual probability of 0.02 corresponding to a return period of 50 years; Figure 6a), the tsunami hazard is concentrated in the eastern Mediterranean. Especially SW Greece and Crete, the south Aegean and Cyprus, NW Egypt and NE Libya, and SE Italy are affected, and PCTA up to about 1 m can be expected at this probability level.

[25] On longer time scales (e.g., an annual probability of 0.0002 corresponding to 5000 years return period; Figure 6c), the entire Mediterranean region is affected by the tsunami hazard. Again the highest hazard is in the eastern Mediterranean, where waves exceeding 5 m can be expected in many places. However, other regions are also strongly affected by the tsunami hazard at low probabilities, especially NW Africa, SE Spain and the Balearic Islands in the western Mediterranean, as well as the Aegean and Marmara Sea regions. The largest expected PCTA with an annual probability of 0.0002 is well above 10 m in northern Libya and southwestern Greece.

[26] An alternative representation of the hazard maps is in terms of the probability of exceeding a given PCTA in a fixed time. Such maps are presented for different wave heights and time frames in Figure 7. It is found that on short time scales (1 year), even small tsunamis have relatively low probability, nowhere exceeding a few percent. The probability of experiencing tsunami events increases with increasing time frame, and on a 100 year scale few sites in northern Libya have up to ~20% probability of experiencing a 5 m tsunami (Figure 7c),

demonstrating the large tsunami potential in the Mediterranean region. Tsunamis up to 10 m have low probability, even on relatively long time scales.

[27] The overall regional tsunami hazard is presented in Figure 8, where we show the probabilities of exceeding different PCTAs at one or more forecast sites in a fixed time period of 1, 30, or 100 years. These curves underline the severity of Mediterranean tsunami hazard with a ~3% probability of exceeding 10 m PCTA in the next 100 years, and more than 90% probability of exceeding 5 m PCTA in the next 30 years.

[28] The results presented in Figure 8 allow for evaluating the tsunami potential of the different source zones. We illustrate this tsunami potential for a range of PCTAs in Figure 9. Assuming a fixed PCTA, the probability is shown of the corresponding tsunami wave being generated in the different source zones. Figure 9 shows that the very large tsunamis (PCTA ≥ 5 m) are almost entirely caused by strong earthquakes in the Hellenic Arc. For the smaller PCTAs the Hellenic Arc is dominating the hazard as well, but also other sources contribute significantly to the hazard, especially the Aegean Sea, Western Albania, Northern Algeria, Sicily, Calabria and the Marmara Sea. It is important to keep in mind, that although, for example, the Northern Algeria and Sicily source zones have relatively low tsunami potential in comparison to the Hellenic Arc, these sources are controlling the hazard in the western Mediterranean where tsunami waves generated in the Hellenic Arc do not reach. In this respect, these sources must be allocated sufficient attention when building up a warning system in the region.

4. Deaggregation

[29] The described PTHA is a very useful tool for assessing the overall hazard posed by tsunamis. However, the
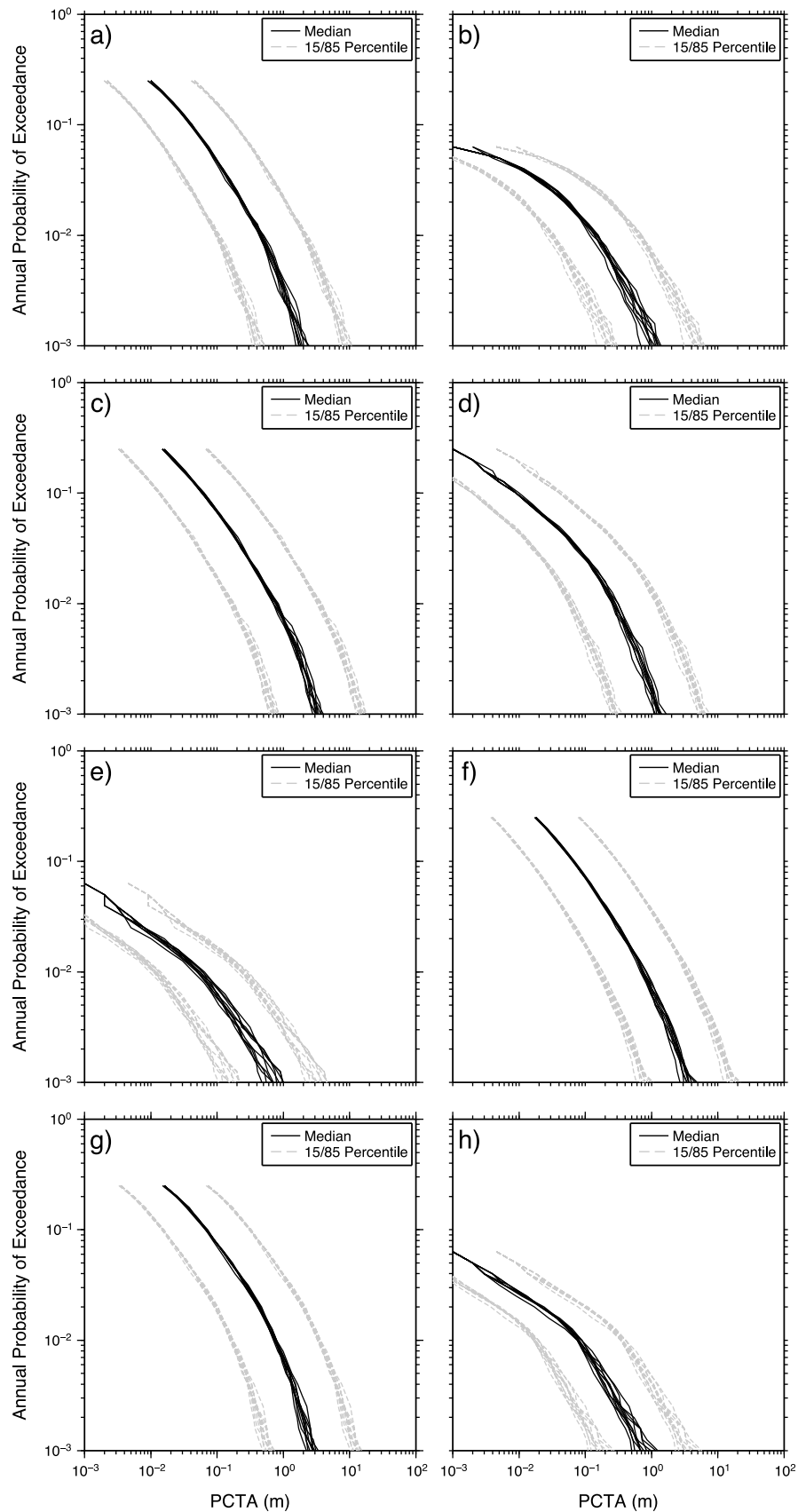
Figure 5. Stability test of hazard curves for selected sites: (a) Alexandria, (b) Istanbul, (c) Athens, (d) Corinth, (e) Nice, (f) Heraklion, (g) Messina, and (h) Mallorca. Hazard curves derived for 10 realizations of the synthetic catalog with 10,000 years duration are shown with their 15th and 85th percentiles.
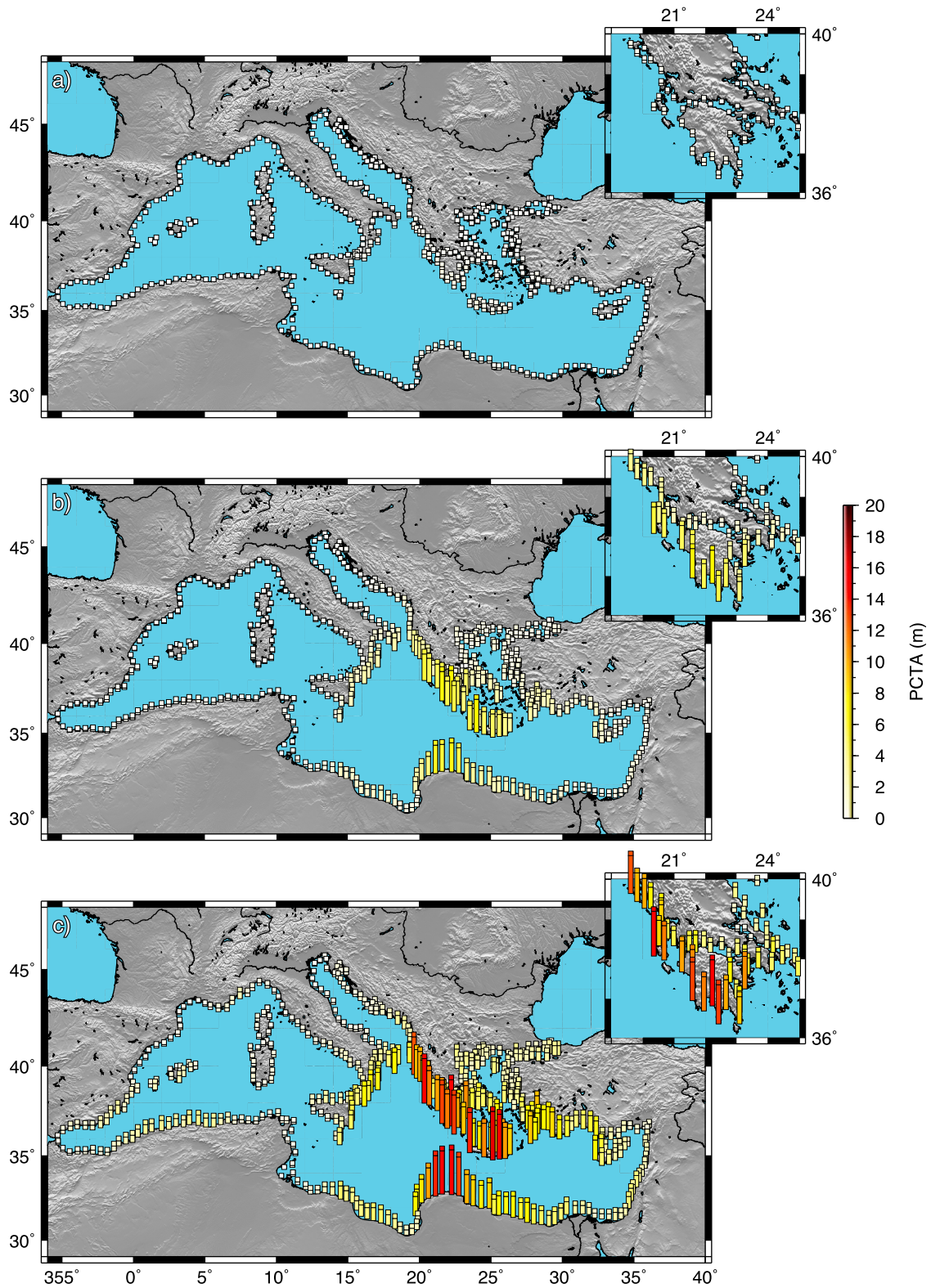
Figure 6. Probabilistic tsunami hazard maps for the Mediterranean region showing tsunami heights with annual probabilities of occurrence of (a) 0.02, (b) 0.002, and (c) 0.0002, corresponding to average return periods of 50, 500 and 5000 years, respectively.
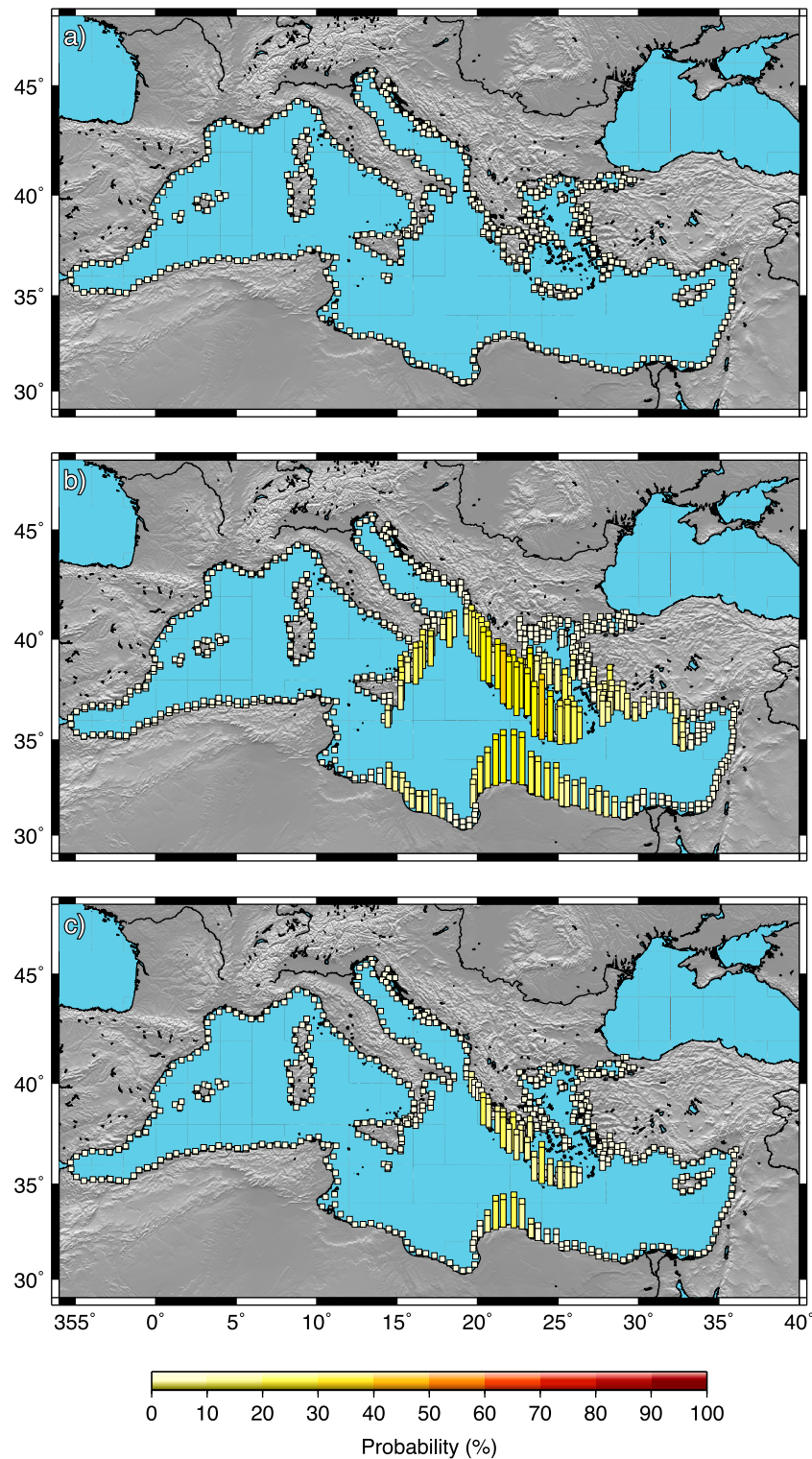
Figure 7. Tsunami hazard represented as the probability of experiencing a tsunami wave with a fixed height in a fixed time period: (a) 1 m PCTA in 1 year, (b) 1 m PCTA in 30 years, and (c) 5 m PCTA in 100 years.

current approach requires computation of thousands of tsunami propagation scenarios and is not suited for detailed (nonlinear) high-resolution inundation studies. Deaggregation of the tsunami hazard into source zones (and other relevant source parameters such as magnitude) allows identification of high-hazard sources affecting a given site, and these sources can then be studied in more detail with high-resolution scenario modeling. In contrast to earlier modeling efforts, such scenarios are firmly based on a probabilistic analysis and do not represent some subjectively defined
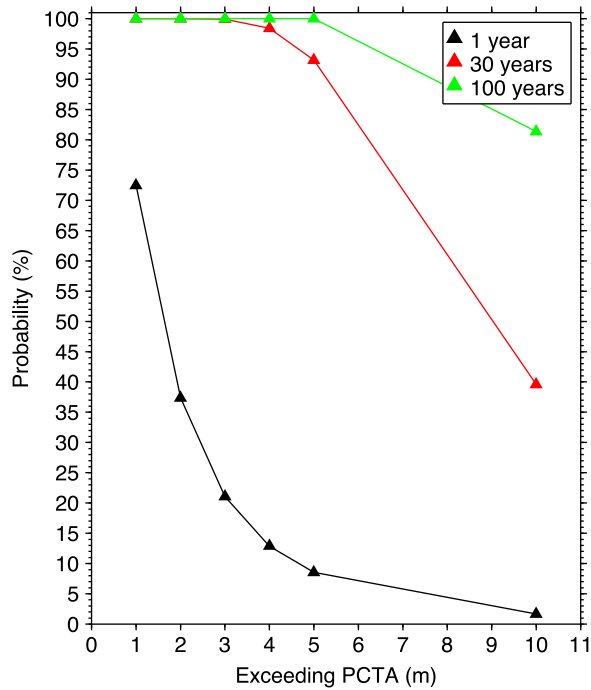
Figure 8. Tsunami hazard represented as the probability of exceeding different wave heights at some location in the Mediterranean in fixed time periods of 1, 30, and 100 years.

maximum credible events, but instead events with known probabilities of occurrence.

[30] By specifying a fixed annual probability level, the source zones contributing to the hazard at a selected site are identified. The results of the deaggregation depend on the site of interest and the selected probability level. For the PTHA deaggregation we determined the median PCTA value for the selected annual probability at the site of interest.

The determined median PCTA and its standard deviation were compared to the synthetic tsunami wave propagation scenarios. If a simulated PCTA was within the range mean ± standard deviation, we extracted the location of the source of the earthquake producing this tsunami wave. Following, the percentage of contribution to the hazard from each source zone was determined. Examples are presented for selected sites in Figure 10, where the main contributors to the hazard at Mallorca, Istanbul, Messina and Alexandria for an annual probability of 0.001 are shown. The results are presented also for additional sites in Table 3. We confirm that the tsunami hazard is mainly controlled by earthquakes in the Hellenic Arc for the eastern Mediterranean, whereas in the western Mediterranean the main contributors are the events along the North Algerian coast and around Sicily and Calabria. The Strait of Sicily acts as an efficient barrier for traveling tsunamis, implying that there is no exchange of tsunami waves between the eastern and the western Mediterranean. In addition to the main contributors, local sources can contribute significantly to the hazard at individual sites. The zones contributing to the hazard at a given site are the same at all probability levels, though the relative contributions of the zones may vary with annual probability.

[31] The deaggregation results show that in most cases, the hazard at a given site is controlled by no more than a few source zones. This has implications for the potential warning times available for a future early warning system in the region. On the basis of the deaggregation results, we have calculated the ranges of tsunami wave travel times between a given site and the source zones contributing to its hazard (Figure 10 and Table 3). The source zones were populated with regularly spaced tsunami point sources at 0.5° grid spacing. The point sources were defined as symmetrical cosine-shaped initial wave elevation with 1 m amplitude and 30 km radius. Arrival times from the point sources at a given point of interest were following calculated, and the minimum and maximum travel times were extracted.
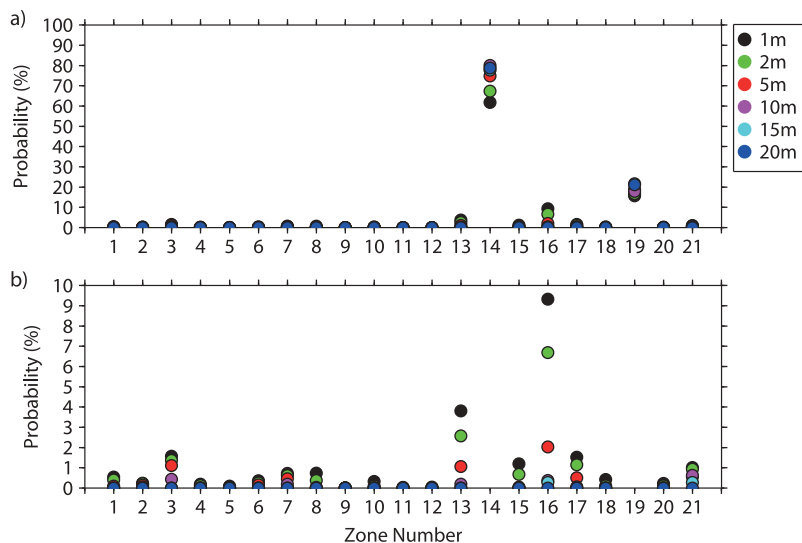
Figure 9. Tsunami potential of the different source zones (a) for the full probability range and (b) zoomed at the low probability levels. Given a fixed tsunami wave height, the probability of the wave being generated in the given source zone is shown. Zone numbers refer to Figure 1.
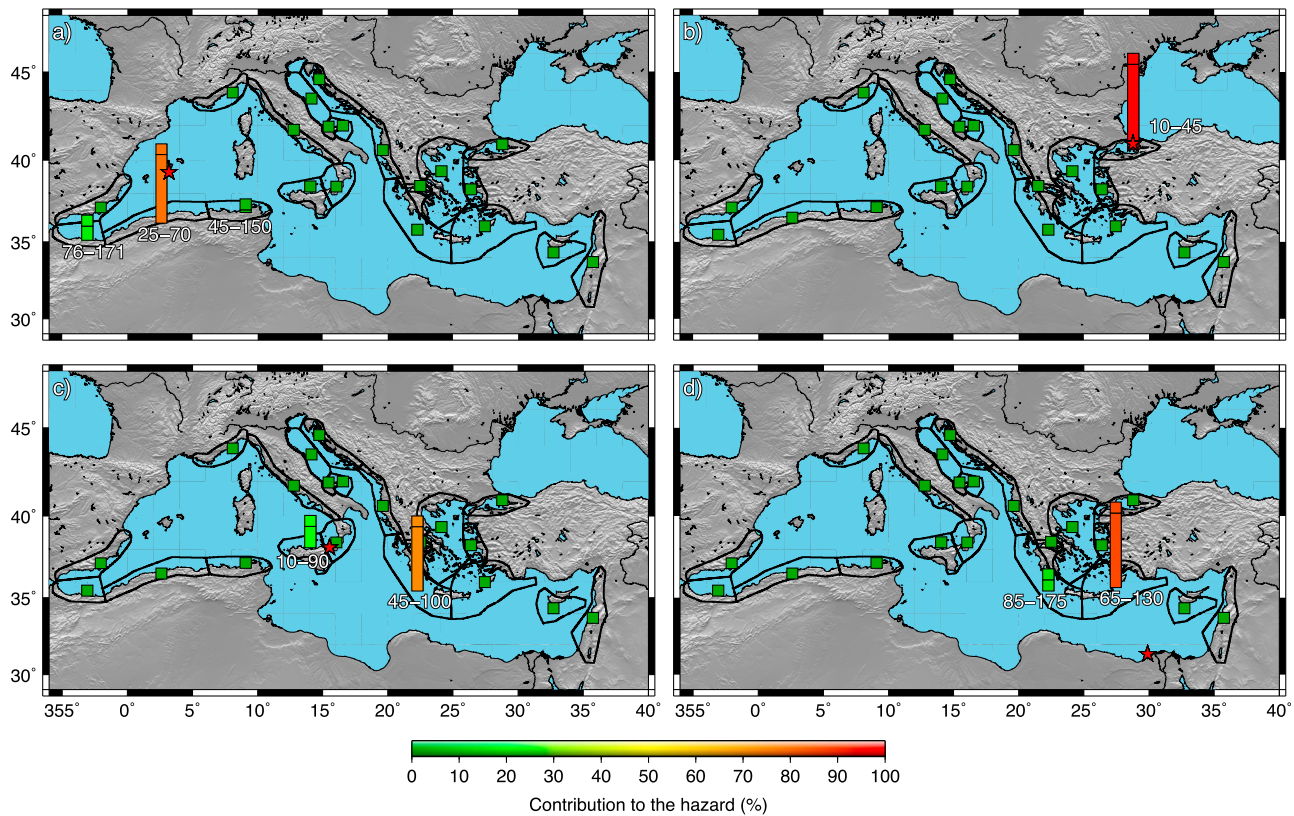
Figure 10. Deaggregation for the sites (a) Mallorca, (b) Istanbul, (c) Messina, and (d) Alexandria, derived for the PCTA with an annual probability of occurrence of 0.001. Numbers indicate the range of travel times (in minutes) for a tsunami wave generated in a given zone to the site of interest.

[32] The travel time results show that there is large geographical variation in the time available for issuing a tsunami warning. For example, in the Marmara Sea where all tsunamis are generated by local earthquakes, travel times vary between a few and ~45 minutes, depending on the location of the earthquake. At the high-hazard sites along the north Egyptian and Libyan coastlines, the tsunami hazard is completely due to earthquakes along the Hellenic Arc. The distance between the coasts of Egypt and Libya and the Hellenic Arc implies that some time will pass before a tsunami reaches these sites. For example, for Darnah which has the highest hazard in this study, a minimum travel time of ~30 minutes is obtained for events in the western part of the Hellenic Arc. For Alexandria, the minimum travel time is ~65 min, making timely tsunami warning feasible. A number of sites are influenced by both local and more distant tsunami sources, and for these the location of the tsunamigenic event will determine the feasibility of tsunami warning. For example, in Messina local earthquakes allow relatively little time for issuing warnings, whereas events in the Hellenic Arc will allow at least 45 min. In this case it is important to note, that although the Hellenic Arc is found to be the main contributor to the tsunami hazard in Messina, history has shown (e.g., with the 1908 event, for which there is an ongoing debate of whether it is earthquake- or landslide-generated [e.g., *Billi et al.*, 2009; *Favalli et al.*, 2009]) that the more infrequent, locally generated tsunamis may cause severe destruction. Some locations, such as the Balearic Islands, are only influenced by distant sources; for example in southern

Mallorca the minimum tsunami travel time is close to 25 min. In summary, many forecast points have at least 20–30 min tsunami travel times, which makes it feasible to

Table 3. Deaggregation Percentages and Corresponding Warning Times

Site of Interest	Zone	Percent Contribution to Hazard[a]	t_{min} (min)	t_{max} (min)
Darnah	Western Hellenic Arc	100	30	105
Alexandria	Eastern Hellenic Arc	87	65	130
	Western Hellenic Arc	13	85	175
Istanbul	Marmara Sea	100	10	45
Athens	Aegean Sea	12	10	170
	Eastern Hellenic Arc	13	60	160
	Western Hellenic Arc	75	55	155
Corinth	Gulf of Corinth	27	5	60
	Western Hellenic Arc	73	70	185
Nice	Northern Morocco	4	134	178
	Northern Algeria	29	75	140
	Northern Tunisia	46	70	135
	Ligurian Coast	21	5	65
Heraklion	Eastern Hellenic Arc	40	10	80
	Western Hellenic Arc	60	15	150
Messina	Sicily	25	10	90
	Western Hellenic Arc	75	45	100
Mallorca	Northern Morocco	17	76	171
	Northern Algeria	80	25	70
	Northern Tunisia	3	45	150

[a]For 0.001 annual probability.

provide timely tsunami warnings for at least parts of the Mediterranean coastline.

5. Discussion

[33] Determining the likelihood of a disaster is a key component of any comprehensive hazard assessment. This is particularly true for tsunamis, even though most tsunami hazard assessments have in the past relied on scenario or deterministic type models. We believe that scenario mode determination of tsunami hazard, while certainly useful, is not sufficient, because it does not allow societies to make risk-based decisions on the basis of quantitative cost/benefit analyses for multiple hazards. In addition, PTHA allows for the integration of multiple tsunami sources in a regional analysis and is a proven mechanism to systematically treat uncertainties in knowledge.

[34] The described methodology for studying the tsunami hazard of the Mediterranean region has the advantage of providing an overall probabilistic hazard estimate for the entire region. The price for this regional coverage is in the reduced degree of detail in the final result. This is associated both with the coarse nature of tsunami source zones and with the rougher bathymetry model which may necessarily be used when calculating tsunami propagation scenarios for such a large number of events. It is important to underline that owing to the relatively coarse grid applied, our results do not account for local coastal effects and they should not be used, for example, in detailed land use planning. However, we present information about the relative distribution of hazard in the region and associate the different coastal tsunami amplitudes with a probability of occurrence. The computed tsunami wave travel times are also largely independent of local wave height. Regional PTHA studies such as the one we present here for the Mediterranean region serve as a reference and input for future local studies. Only when combining both elements, tsunami risk assessment can best serve the needs of societies.

[35] Another consequence of the coarse zonation is that the faulting regimes and event depths defined for a given source zone may not represent the seismicity well for parts of the zone. In many cases, a specific faulting mechanism or event depth range will only be expected within a part of the source zone, and this may lead to unlikely events in the synthetic catalogue. Whereas this issue will need to be addressed in future studies, the test performed in Figure 5 indicates that the effect of this uncertainty in the faulting mechanisms on the hazard results is limited. Considering that most events in the synthetic catalog are shallow, we expect a similarly limited effect of the event depth uncertainty.

[36] Ideally, our results should have been validated through a comparison to a complete catalog of recorded tsunamis. Unfortunately, existing tsunami catalogs for the Mediterranean region are largely incomplete, and only a rough comparison can be made. In the GITEC-TWO catalog [Tinti et al., 2001], 34 relatively reliable earthquake generated tsunamis (reliability factor 3 or 4) are listed in the Mediterranean Sea in the 20th century. Of these, only 13 are listed with a corresponding wave height that we assume to be the maximum observed. Eight of the events are listed with a maximum wave height of 1 m or more; three of these exceed 10 m wave height. Considering this, the results of this study

seem to be in general agreement with the observed tsunami history of the last century. Another test is whether events that have occurred in the past are also found in the synthetic catalog. This is indeed the case, for example several of the events in the synthetic catalog generate tsunamis with wave heights exceeding 25 meters in the Aegean Sea as was observed for the 1956 tsunami [Papazachos et al., 1985].

[37] Also a direct comparison of our results to previous estimates of tsunami hazards is not straightforward, mainly for two reasons. Firstly, previous tsunami hazard studies for the Mediterranean region are mainly scenario-based and consider worst case or most credible scenarios, without a clearly defined probability of occurrence. Secondly, the wave height definition and detail in estimation of inundation varies from study to study. Therefore, only a qualitative comparison to the results of previous studies will be given in the following. Lorito et al. [2008] considered the tsunami hazard in Southern Italy due to most credible scenarios from three tsunamigenic earthquake sources. Their findings are in general agreement with our results: The largest tsunami hazard in Southern Italy is found to be due to earthquakes in the Eastern Hellenic Arc where tsunami waves up to ~4 m can affect Sicily. This is slightly above our results for 0.002 annual probability, and slightly lower than our results for 0.0002 annual probability. In southern mainland Italy, Lorito et al. [2008] find, as in this study, that the largest tsunami hazard is toward the Ionian Sea, with much smaller wave heights in the Tyrrhenian Sea. For Sardinia, the hazard is found to be lower, with maximum wave heights around 1.5 meters, which agrees well with the maximum PCTA found in this study. Tinti et al. [2005] studied the tsunami hazard in Sicily and Calabria using a hybrid statistical-deterministic method. They found the expected number of tsunami waves exceeding 1 m within 10,000 years for a number of 0.25° × 0.25° cells. For the cell containing Messina, 6.3–12.4 occurrences are expected, corresponding to an annual probability in the range 0.00063–0.00124. We find an annual probability of exceeding 1 m PCTA in Messina of 0.007, which indicates a higher hazard level than that found by Tinti et al. [2005]. Tiberti et al. [2008] study the tsunami hazard along the Italian Adriatic coastline through scenarios of tsunamis generated by most credible earthquakes in six source zones. They find a low tsunami hazard in the northern Adriatic, increasing toward the south, though in most places only waves smaller than 1 m are expected. In the present study we find larger tsunami hazard along the southern Italian Adriatic coast than what is found by Tiberti et al. [2008], most likely because that study does not consider tsunamis generated in the eastern Hellenic Arc, which is expected to be an important contributor to the tsunami hazard in that region. For the Marmara Sea, Hébert et al. [2005] have studied a number of earthquake scenarios with magnitudes up to 7.6 along the North Anatolian Fault. They find that tsunamis generated by earthquakes alone can lead to waves up to 2 m on the coast. This fits well with our results for Istanbul, but is slightly lower than our maximum PCTA values in the Marmara Sea for the lowest probability levels. Salamon et al. [2007] study tsunami hazard along the Levant coast in the easternmost Mediterranean in terms of landslide and earthquake generated tsunami scenarios. They find that in this region, landslides generate more severe tsunamis, and that earthquake generated tsunamis are limited

to wave heights of up to 1–3 m. This is in good agreement with the maximum PCTA values found for the Levant coast in this study. For a larger region in the eastern Mediterranean, *Papadopoulos et al.* [2007] consider the observed tsunami history and find a mean recurrence of strong tsunamis (maximum wave height exceeding ∼4 m) of ∼142 years. Comparable tsunami waves are found in our hazard map for 0.02 annual probability (corresponding to a mean return period of 500 years), indicating a lower hazard level than that found by *Papadopoulos et al.* [2007]. There are two likely explanations for this discrepancy. Firstly, the results of *Papadopoulos et al.* [2007] give the probabilities of tsunamis occurring somewhere in the eastern Mediterranean, whereas our results are for individual sites. Secondly, the observed catalog may contain tsunamis generated by submarine slides triggered by earthquake ground shaking. Such events are not included in the present study.

[38] One innovative component of our PTHA implementation when compared to earlier such studies [e.g., *Geist and Parsons*, 2006; *Power et al.*, 2007; *Thio et al.*, 2007] is the deaggregation of our results in both space and time (Figure 10). Through the deaggregation we identify the main contributors to the hazard at a given site, which can again be used for defining critical deterministic scenarios to be studied in more detail. The advantage of this approach is that the scenarios can be associated directly with a probability of occurrence. The deaggregation in time is a critical component of the hazard assessment as it provides important information about the time available to issue a tsunami warning in a potential future warning system. This can contribute to the development of a more efficient warning system, both in terms of warning time and the cost of deployment and maintenance.

[39] There are a number of issues related to our implementation, which we would like to improve in the future to obtain better constrained hazard estimates. These include associating the largest earthquakes to predefined structures to avoid large events with unrealistic rupture orientations, calibrating activity rates and faulting regimes on the basis of geodetic strain rates, defining complex slip models for earthquakes in the catalog instead of using the simple uniform slip assumption and a more extensive treatment of uncertainties in all steps of the calculation. It is furthermore desirable to include a higher level of detail in the tsunami propagation scenarios. Much of the information required for doing these improvements is currently being compiled for the Mediterranean region and can be implemented in the future. For example, the SHARE project (www.share.eu.org) is working on a new harmonized seismic hazard model for the Euro-Mediterranean region, which could readily replace the model we derived (Figure 1 and Table 2) in future PTHA studies. Also, some of these issues can be dealt with more easily for an implementation on a more local scale.

6. Conclusions

[40] We present the first probabilistic estimate of tsunami hazard in the Mediterranean Sea, showing that the entire region is prone to devastating tsunami events (e.g., Figure 6). Highest hazard is found in the eastern Mediterranean where peak coastal tsunami amplitudes (PCTA) exceeding 10 m can be expected on a 5000 year time scale

(Figure 6c). In the western Mediterranean, the hazard is lower, but tsunami waves exceeding 1 m are possible at most locations. The deaggregation of the results (Figure 10) shows that the main contributor to the hazard is the Hellenic Arc, but that also other sources may be important for the hazard on a more local scale. This study has considered only earthquake-generated tsunamis, and other sources, such as landslides and volcanic eruptions, will contribute further to the hazard in the region. Considering the high level of tsunami hazard presented in this study, it is urgent that a tsunami warning system is developed and implemented in the Mediterranean region. Because the Hellenic Arc and the northern Maghreb region are the most likely tsunamigenic regions and also offer the longest time to issue a warning, we recommend focusing the initial efforts toward a tsunami early warning system especially on these source regions.

References

Alasset, P.-J., H. Hébert, S. Maouche, V. Calbini, and M. Meghraoui (2006), The tsunami induced by the 2003 Zemmouri earthquake (M_w = 6.9, Algeria): Modelling and results, *Geophys. J. Int.*, 166(1), 213–226, doi:10.1111/j.1365-246X.2006.02912.x.

Billi, A., L. Minelli, B. Orecchio, and D. Presti (2009), Runup distribution for the 1908 Messina tsunami in Italy: Observed data versus expected curves, *Bull. Seismol. Soc. Am.*, 99, 3502–3509, doi:10.1785/0120090128.

Budnitz, R. J., G. Apostolakis, D. M. Boore, L. S. Cluff, K. J. Coppersmith, C. A. Cornell, and P. A. Morris (1997), Recommendations for probabilistic seismic hazard analysis: Guidance on uncertainty and use of experts, *Rep. NUREG/CR-6372*, U.S. Nucl. Regul. Comm., Washington, D. C.

Cornell, C. A. (1968), Engineering seismic risk analysis, *Bull. Seismol. Soc. Am.*, 58, 1583–1606.

Cosentino, P., V. Ficarra, and D. Luzio (1977), Truncated exponential frequency-magnitude relationship in earthquake statistics, *Bull. Seismol. Soc. Am.*, 67, 1615–1623.

DISS Working Group (2009), A compilation of potential sources for earthquakes larger than M 5.5 in Italy and surrounding areas, Database of Individual Seismogenic Sources, Version 3.1.0, http://diss.rm.ingv.it/diss/, Ist. Naz. di Geofis. e Vulcanol., Rome.

Electric Power Research Institute (1994), The earthquakes of stable continental interiors: Assessment of large earthquake potential, vol. 1, *Rep. TR-102261 s-V1–V5*, Electr. Power Res. Inst., Palo Alto, Calif.

Favalli, M., E. Boschi, F. Mazzarini, and M. T. Pareschi (2009), Seismic and landslide source of the 1908 Straits of Messina tsunami (Sicily, Italy), *Geophys. Res. Lett.*, 36, L16304, doi:10.1029/2009GL039135.

Friedrich, W. L., B. Kromer, M. Friedrich, J. Heinemeier, T. Pfeiffer, and S. Talamo (2006), Santorini eruption radiocarbon dated to 1627–1600 B.C., *Science*, 312, 548, doi:10.1126/science.1125087.

Geist, E. L., and T. Parsons (2006), Probabilistic analysis of tsunami hazards, *Nat. Hazards*, 37, 277–314, doi:10.1007/s11069-005-4646-z.

Hébert, H., F. Schindelé, Y. Altinok, B. Alpar, and C. Gazioglu (2005), Tsunami hazard in the Marmara Sea (Turkey): A numerical approach to discuss active faulting and impact on the Istanbul coastal areas, *Mar. Geol.*, 215, 23–43, doi:10.1016/j.margeo.2004.11.006.

Intergovernmental Oceanographic Commission (1997), IUGG/IOC Time Project: Numerical method of tsunami simulation with the leap-frog scheme, in *IOC Manuals Guides*, vol. 35, 126 pp., U. N. Educ., Sci., and Cult. Organ., Paris.

Kamigaichi, O. (2009), Tsunami forecasting and warning, in *Encyclopedia of Complexity and System Science*, pp. 9592–9617, Springer, New York.

Lorito, S., M. M. Tiberti, R. Basili, A. Piatanesi, and G. Valensise (2008), Earthquake-generated tsunamis in the Mediterranean Sea: Scenarios of potential threats to Southern Italy, *J. Geophys. Res.*, 113, B01301, doi:10.1029/2007JB004943.

Okada, Y. (1985), Surface deformation due to shear and tensile faults in a half-space, *Bull. Seismol. Soc. Am.*, 75, 1135–1154.

Papadopoulos, G. A., and A. Fokaefs (2005), Strong tsunamis in the Mediterranean Sea: A re-evaluation, *ISET J. Earthquake Technol.*, 42, 159–170.

Papadopoulos, G. A., E. Daskalaki, A. Fokaefs, and N. Giraleas (2007), Tsunami hazards in the Eastern Mediterranean: Strong earthquakes and tsunamis in the East Hellenic Arc and Trench system, *Nat. Hazards Earth Syst. Sci.*, 7, 57–64, doi:10.5194/nhess-7-57-2007.

Papazachos, B. C., C. Koutitas, P. M. Hatzidimitriou, B. G. Karacostas, and C. A. Papaioannou (1985), Source and short-distance propagation of the July 9, 1956 Southern Aegean tsunami, *Mar. Geol.*, 65, 343–351, doi:10.1016/0025-3227(85)90064-7.

Paulatto, M., T. Pinat, and F. Romanelli (2007), Tsunami hazard scenarios in the Adriatic Sea domain, *Nat. Hazards Earth Syst. Sci.*, 7, 309–325, doi:10.5194/nhess-7-309-2007.

Power, W., G. Downes, and M. Stirling (2007), Estimation of tsunami hazard in New Zealand due to South American earthquakes, *Pure Appl. Geophys.*, 164, 547–564, doi:10.1007/s00024-006-0166-3.

Reiter, L. (1990), *Earthquake Hazard Analysis*, Columbia Univ. Press, New York.

Salamon, A., T. Rockwell, S. N. Ward, E. Guidoboni, and A. Comastri (2007), Tsunami hazard evaluation of the Eastern Mediterranean: Historical analysis and selected modeling, *Bull. Seismol. Soc. Am.*, 97, 705–724, doi:10.1785/0120060147.

Shaw, B., N. N. Ambraseys, P. C. England, M. A. Floyd, G. J. Gorman, T. F. G. Higham, J. A. Jackson, J.-M. Nocquet, C. C. Pain, and M. D. Piggott (2008), Eastern Mediterranean tectonics and tsunami hazard inferred from the AD 365 earthquake, *Nat. Geosci.*, 1, 268–276, doi:10.1038/ngeo151.

Shuto, N. (1991), Numeric simulation of tsunamis: Its present and near future, *Nat. Hazards*, 4, 171–191, doi:10.1007/BF00162786.

Soloviev, S. L. (1990), Tsunamigenic zones in the Mediterranean Sea, *Nat. Hazards*, 3, 183–202, doi:10.1007/BF00140432.

Thio, H. K., P. Somerville, and G. Ichinose (2007), Probabilistic analysis of strong ground motion and tsunami hazard in Southeast Asia, *J. Earthquake Tsunami*, 1(2), 119–137, doi:10.1142/S1793431107000080.

Tiberti, M. M., S. Lorito, R. Basili, V. Kastelic, A. Piatanesi, and G. Valensise (2008), Scenarios of earthquake-generated tsunamis for the Italian coast of the Adriatic Sea, *Pure Appl. Geophys.*, 165, 2117–2142, doi:10.1007/s00024-008-0417-6.

Tinti, S., and A. Armigliato (2003), The use of scenarios to evaluate tsunami impact in southern Italy, *Mar. Geol.*, 199, 221–243, doi:10.1016/S0025-3227(03)00192-0.

Tinti, S., A. Maramai, and L. Grazziani (2001), A new version of the European tsunami catalogue: Updating and revision, *Nat. Hazards Earth Syst. Sci.*, 1, 255–262, doi:10.5194/nhess-1-255-2001.

Tinti, S., A. Armigliato, R. Tonini, A. Maramai, and L. Graziani (2005), Assessing the hazard related to tsunamis of tectonic origin: A hybrid statistical-deterministic method applied to Southern Italy coasts, *ISET J. Earthquake Technol.*, 42, 189–201.

Weichert, D. H. (1980), Estimation of the earthquake recurrence parameters for unequal observation periods for different magnitudes, *Bull. Seismol. Soc. Am.*, 70, 1337–1346.

Wells, D. L., and K. J. Coppersmith (1994), New empirical relationships among magnitude, rupture length, rupture width, rupture area, and surface displacement, *Bull. Seismol. Soc. Am.*, 84, 974–1002.

Wiemer, S., D. Giardini, D. Fäh, N. Deichmannm, and S. Sellami (2009), Probabilistic seismic hazard assessment of Switzerland, *J. Seismol.*, 13, 449–478, doi:10.1007/s10950-008-9138-7.

A. Babeyko and G. Grünthal, GFZ German Research Centre for Geosciences, Telegrafenberg, D-14473 Potsdam, Germany.

M. B. Sørensen, Department of Earth Science, University of Bergen, Allegt. 41, N-5007 Bergen, Norway. (mathilde.sorensen@geo.uib.no)

M. Spada and S. Wiemer, Swiss Seismological Service, ETH Zürich, Sonneggstrasse 5, CH-8092 Zürich, Switzerland.